

WinkTPG: An Execution Framework for Multi-Agent Path Finding Using Temporal Reasoning

Jingtian Yan, Stephen F. Smith, Jiaoyang Li

Carnegie Mellon University
jingtianyan@cmu.edu, sfs@cmu.cs.edu, jiaoyangli@cmu.edu

Abstract

Planning collision-free paths for a large group of agents is a challenging problem with numerous real-world applications. While recent advances in Multi-Agent Path Finding (MAPF) have shown promising progress, standard MAPF algorithms rely on simplified kinodynamic models, preventing agents from directly following the generated MAPF plan. To bridge this gap, we propose kinodynamic Temporal Plan Graph Planning (kTPG), a multi-agent speed optimization algorithm that efficiently refines a MAPF plan into a kinodynamically feasible plan while accounting for uncertainties and preserving collision-freeness. Building on kTPG, we propose Windowed kTPG (WinkTPG), a MAPF execution framework that incrementally refines MAPF plans using a window-based mechanism, dynamically incorporating agent information during execution to reduce uncertainty. Experiments show that WinkTPG can generate speed profiles for up to 1,000 agents in 1 second and improves solution quality by up to 51.7% over existing MAPF execution methods.

1 Introduction

Coordinating agents without collisions is important for applications in scenarios like automated warehouses (Wurman, D’Andrea, and Mountz 2008), traffic intersections (Li et al. 2023), and airports (Morris et al. 2016). Multi-Agent Path Finding (MAPF) methods offer significant advantages for solving this problem, such as scalability and (bounded) optimality guarantees. Yet, applying MAPF in these domains remains challenging: most MAPF methods ignore real-world factors like kinodynamics (e.g., speed and acceleration limits) and uncertainty (e.g., execution delay), making it impractical for agents to strictly follow the planned paths.

One promising solution is to postprocess the plan generated by MAPF methods. Hönig et al. [2016] introduce Temporal Plan Graph (TPG), which refines the speed profiles of agents to meet their speed limits while preserving the passing orders of agents at different locations. While TPG ensures collision-free and deadlock-free, it cannot handle kinodynamic constraints beyond speed limits. That is, it may generate speed profiles with infinitely large accelerations, making them infeasible for agents to follow. Two extensions of TPG overcome this issue: Kinodynamic Network

(KDN) (Zhang et al. 2021) and Action Dependency Graph (ADG) (Hönig et al. 2019). KDN incorporates kinodynamic constraints into TPG but suffers from limited scalability and cannot handle uncertainty. In contrast, ADG is a distributed execution framework using TPG that lets each agent plan its speed profile. However, as we later show, ADG is conservative, frequently forcing agents to decelerate unnecessarily.

To overcome this limitation, we propose **Windowed Kinodynamic Temporal Plan Graph** planning (WinkTPG), an efficient execution framework for MAPF. Given a set of collision-free paths, we use a TPG to encode their passing orders at different locations. Instead of taking the conservative strategy used by ADG, WinkTPG uses our proposed kinodynamic planner, kTPG, to plan speed profiles that leverage the movement capabilities of agents to avoid unnecessary deceleration. Specifically, kTPG first transforms the passing order constraints into reserved time intervals, during which agents must traverse specific locations. Then, for each agent, kTPG generates a speed profile that satisfies both reserved intervals and kinodynamic constraints. To ensure the safety of those speed profiles with respect to execution time uncertainty, we add a safety margin mechanism to kTPG. Moreover, WinkTPG uses a windowed mechanism to enhance robustness and efficiency during execution. This mechanism uses updated information during execution to reduce uncertainty and improve overall performance through dynamic replanning. Theoretically, we prove that kTPG and WinkTPG are complete. Empirically, we evaluate them on the standard MAPF benchmark with two robot models and various uncertainty levels. WinkTPG shows up to 51.7% improvement in terms of solution quality compared to ADG. Moreover, WinkTPG generates speed profiles for 1,000 agents within 1 second, whereas KDN requires up to 300 seconds and scales only to 200 agents.

2 Preliminaries

Before describing our approach we first define the MAPF problem and the temporal plan graph that encodes the MAPF plan, and review related works on executing MAPF plans.

2.1 MAPF Problem

As shown in Fig. 1 (a), a MAPF problem (Stern et al. 2019) contains an undirected graph $\mathcal{G}_U = (\mathcal{V}_U, \mathcal{E}_U)$ and I agents $\mathcal{A} = \{a_1, \dots, a_I\}$, each with a start $q_i^s \in \mathcal{V}_U$ and goal

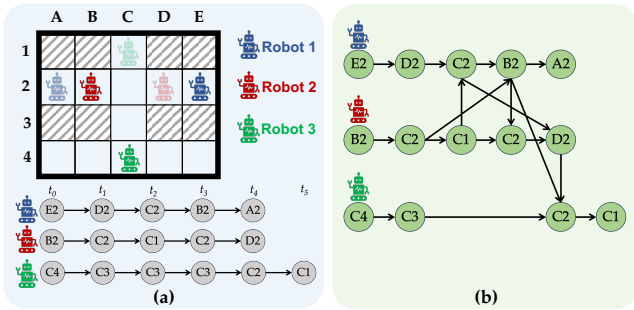


Figure 1: Example of MAPF problem, plan, and a TPG.

$q_i^g \in \mathcal{V}_U$. Time is discretized, and at each timestep, an agent can either move to an adjacent vertex or remain at its current vertex. A MAPF plan is a set of collision-free paths $\mathcal{P} = \{p_1, \dots, p_I\}$, where the path of a_i is a sequence of time-annotated vertices: $p_i = \{(q_i^0, t_0), \dots, (q_i^{z^i}, t_{z^i})\}$. Here, $q_i^0 = q_i^s, q_i^{z^i} = q_i^g, q_i^k \in \mathcal{V}_U$ and $(q_i^{k-1}, q_i^k) \in \mathcal{E}_U$ for all $k \in \{1, \dots, z^i\}$. \mathcal{P} is defined as collision-free if it contains *No vertex collisions* - agents must not occupy the same vertex at the same time, and *No edge collisions* - agents must not swap vertices simultaneously. To avoid confusion with the TPG, we refer to vertices in \mathcal{V}_U as *locations*.

2.2 Temporal Plan Graph (TPG)

A Temporal Plan Graph (TPG), as shown in Fig. 1 (b), is a directed acyclic graph $\mathcal{G} = (\mathcal{V}, \mathcal{E}_1, \mathcal{E}_2)$ that represents a MAPF plan by capturing precedence relationships for visiting locations. The vertex set $\mathcal{V} = \{v_i^k : k \in [0, z^i], a_i \in \mathcal{A}\}$ comprises all locations to be visited sequentially by agent a_i (i.e., $loc(v_i^k) \in \mathcal{V}_U$). The edge set \mathcal{E}_1 includes *Type-1 edges*, which capture sequential precedence within the path of an agent. A Type-1 edge (v_i^k, v_i^{k+1}) ensures that a_i visits v_i^k before v_i^{k+1} . The edge set \mathcal{E}_2 consists of *Type-2 edges*, which enforce the order in which agents visit shared locations. For any two vertices v_j^s and v_i^k such that $loc(v_j^s) = loc(v_i^k)$, a Type-2 edge (v_j^{s+1}, v_i^k) ensures that a_i can enter v_i^k only after a_j leaves v_j^s and reaches v_j^{s+1} .

2.3 Related Works

MAPF methods have been developed to find collision-free paths for a large group of agents. Leading methods, such as EECBS (Li, Ruml, and Koenig 2021), PIBT (Okumura et al. 2022), and PBS (Ma et al. 2019), can find collision-free paths for thousands of agents. However, these methods assume all agents move synchronously, which is unrealistic in real-world scenarios due to their reliance on simplified kinodynamic models. To address this issue, some methods (Andreychuk et al. 2021; Yan and Li 2024; Moldagalieva et al. 2024) integrate more accurate kinodynamic models during planning. Nevertheless, these methods often face scalability challenges due to the increased computational complexity introduced by the kinodynamic models. Another group of methods (Hönig et al. 2016; Zhang et al. 2021) first generates a MAPF plan with a simplified kinodynamic model and

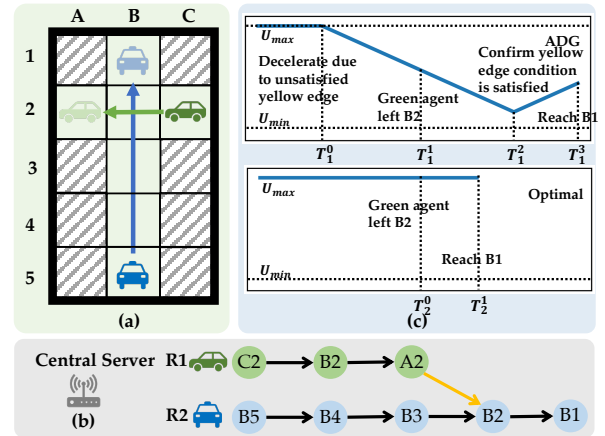


Figure 2: (a) MAPF instance with a green agent (R1) moving from C2 to A2, and a blue agent (R2) moving from B5 to B1. Both agents have an initial speed of U_{max} . (b) TPG generated by the central server, where the yellow edge indicates that R2 can only move to B2 after R1 has left it. (c) ADG-generated and optimal speed profiles for R2.

subsequently derives speed profiles with the accurate model based on these paths. For instance, KDN (Zhang et al. 2021) employs a TPG to encode the passing order constraints defined in the MAPF plan. It then uses a Mixed-Integer Linear Programming (MILP) solver to find kinodynamically feasible speed profiles for agents based on the TPG.

To handle time uncertainty that exists during execution, some methods (Atzmon et al. 2020; Peltzer et al. 2020) account for uncertainty during planning. These methods first build a model of the uncertainty and then plan collision-free paths, ensuring that agents remain collision-free even when time uncertainties occur as described by the models. While effective in some cases, these methods often lead to poor performance due to being overly conservative during the planning stage, as they cannot access the actual delays that occur during execution. Additionally, these methods are often limited in scalability.

Introducing an execution framework to MAPF is a promising approach to meet robot kinodynamic constraints while ensuring robustness. Action Dependency Graph (ADG) (Hönig et al. 2019) uses a TPG to ensure the passing order and defines an execution framework for speed profile generation. Specifically, it categorizes the vertices in the graph into three statuses: *staged*, *enqueued*, and *finished*. A vertex is marked as *staged* if the agent cannot move to it yet. It transitions to *enqueued* when the agent can safely move here. This happens only if it has no preceding vertices or if the following conditions are met: (1) its preceding vertex connected by a Type-1 edge is *enqueued* or *finished*, and (2) all preceding vertices connected by Type-2 edges are *finished*. Once a vertex transitions to *enqueued*, ADG generates a speed profile for the agent to reach the vertex. A vertex is marked as *finished* when the agent has reached it. ADG dynamically updates vertex statuses during execution and provides robustness guarantees under temporal uncertainty.

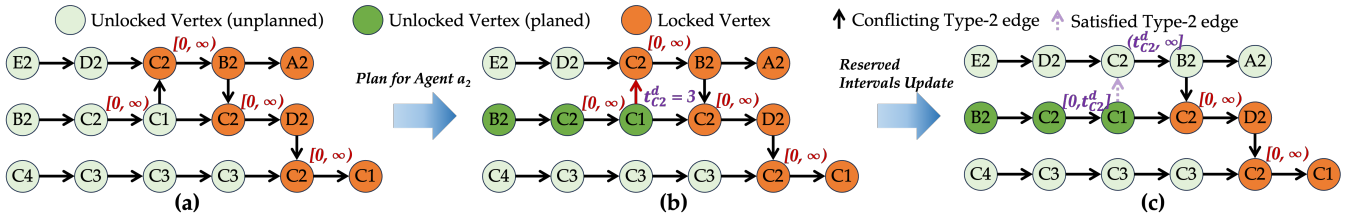


Figure 3: Updating reserved intervals to satisfy the conflicting Type-2 edge from C1 to C2.

However, ADG only plans the speed profile for a vertex after it transitions to *enqueued*, even when it is predictable that this transition will happen before the agent reaches it. This conservative strategy can lead to unnecessary deceleration. As shown in Fig. 2, R2 (blue) must wait until R1 (green) leaves cell B2 before it can proceed. Although it is evident early on that R1 will leave B2 before R2 arrives, ADG does not allow R2 to commit to the optimal speed profile until the dependency is officially satisfied. This results in R2 decelerating prematurely (top chart in (c)), compared to the optimal case (bottom chart) where it could have maintained maximum speed. The problem is worsened by potential communication delays in real-world settings, where agents rely on frequent updates from a central server. Consequently, this overly conservative strategy can result in poor performance in many scenarios.

3 Kinodynamic TPG (kTPG)

Definition 1 below specifies the problem addressed in this section. In Sections 4 and 5, we will extend this definition to account for temporal uncertainty during agent movement.

Definition 1 (Multi-Agent Execution Problem (MAEP))
Given a MAPF plan, the objective of MAEP (Zhang et al. 2021) is to generate a set of speed profiles for all agents to follow during execution. These profiles must satisfy the kinodynamic constraints imposed by the agents' physical models, remain collision-free, and respect the precedence relationships defined in the MAPF plan. The objective is to minimize the total time for all agents to reach their goals.

3.1 kTPG Overview

The precedence constraints in a MAPF plan require that each agent (1) follows its assigned path in sequence and (2) respects the relative passing ordering of shared locations with other agents. These constraints can be encoded in a TPG \mathcal{G} . Assume each agent a_i begins at its start location $q_i^0 = q_i^s$ at time $t = 0$, and its state at time t is defined as $s_i(t) = (q_i^t, \theta_i^t)$, with $q_i^t \in \mathcal{V}_U$ and $\theta_i^t \in \Theta$ being its location and orientation, respectively. We use *reach time* $t_i^r(q_i^k)$ to denote the time when a_i reaches location q_i^k . For ease of reading, we introduce the term *leave time* $t_i^l(q_i^k) = t_i^r(q_i^{k+1})$, i.e., the time when a_i reaches its next location. We say a_i occupies location q_i^k during $[t_i^r(q_i^k), t_i^l(q_i^{k+1})]$. A collision occurs if two agents occupy the same location during overlapping time intervals. We say that the speed profiles *satisfy* the edges in \mathcal{G} if the time intervals during which agents occupy each location (as defined by the speed profiles) do not

violate the precedence constraints imposed by the edges. It is easy to show that satisfying all edges in the TPG guarantees that the precedence constraints defined in the MAPF plan are preserved. The high-level idea of kTPG is to introduce a *reserved interval* constraint on each vertex of the TPG, initialized as $[0, \infty)$. It then generates speed profiles for each agent independently that visit each vertex within its corresponding reserved intervals. kTPG iteratively updates these constraints and the corresponding speed profiles until the reserved intervals of the vertices corresponding to the same location do not overlap, which in turn ensures that the corresponding speed profiles do not lead to collisions.

We use the example in Fig. 3 to show a single iteration of this process. Each iteration begins by selecting an agent to replan, following the selection rule in Section 3.2; in this case, a_2 is selected. We define a Type-2 edge as *satisfied* if the reserved intervals at its associated vertices do not overlap and the visiting order is preserved. Otherwise, it is *conflicting*. All Type-2 edges in our example are conflicting in this iteration. We then generate a speed profile for a_2 from its first to last *unlocked* vertex, i.e., vertices without any incoming conflicting edges, using the method in Section 3.3. These vertices are shown as dark green circles in Fig. 3 (b). Next, we identify the conflicting edges originating from these unlocked vertices (i.e., the red edge in Fig. 3 (b)). We use the generated speed profile to derive a split time for the target vertex (here, C2) and update the reserved intervals for both agents accordingly so that the intervals no longer overlap (see Section 3.4). This update allows us to satisfy a conflicting edge and unlock additional vertices of other agents, as shown in Fig. 3 (c). In the next iteration, we use the newly unlocked vertices to satisfy more Type-2 edges by selecting another agent and updating its speed profile. This process repeats until all Type-2 edges are satisfied, at which point we get complete, collision-free speed profiles for all agents.

3.2 Selecting Agent

The order in which agents are selected for replanning is important. As shown in Fig. 4, if we plan for a_1 first, no additional vertices are unlocked in that iteration. In contrast, planning for a_2 first results in three vertices being unlocked. Thus, the selection order directly affects the number of vertices unlocked per iteration, which in turn influences the total number of iterations required to unlock all vertices. Motivated by this observation, kTPG adopts the following strategy: At each iteration, we select the agent that can satisfy the greatest number of conflicting Type-2 edges originating from its currently unlocked vertices.

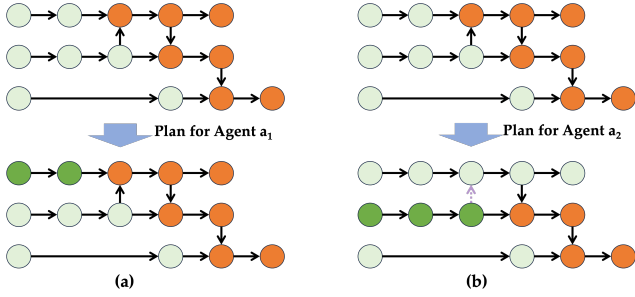


Figure 4: kTPG with agent selection: (a) a_1 first, (b) a_2 first.

3.3 Updating Speed Profile

After selecting an agent, we compute a speed profile that visits each unlocked vertex within its reserved interval, starts and ends with zero speed, and satisfies the robot’s kinodynamic constraints. Because these unlocked vertices have no incoming conflicting edges, the resulting speed profile is guaranteed to be collision-free and can safely be used to update the reserved intervals. This can be accomplished using a single-agent motion planner or speed optimization techniques (Liu, Zhan, and Tomizuka 2017; Ali and Yakovlev 2023). Empirically, we achieve this by using a 1-D adaptation of SIPP-IP (Ali and Yakovlev 2023), an optimal algorithm that performs an A*-type search along the vertices using a set of predefined motion primitives.

3.4 Satisfying Conflicting Edges

After we get the speed profile for a_i , we update the reserved intervals to satisfy conflicting edges. Specifically, for each conflicting edge (v_i^{k+1}, v_j^s) originating from an unlocked vertex v_i^{k+1} of a_i , we use the leave time of a_i at the shared location $loc(v_i^k) = loc(v_j^s)$, denoted as t^l , as the split time to divide the time interval at the shared location into $[0, t^l]$ and (t^l, ∞) . We enforce that a_i and a_j occupy the shared location within these intervals respectively. Concretely, we update the reserved intervals for v_i^k and v_j^s by intersecting them with the corresponding segments.

Fig. 3 shows an example. Once the speed profile for agent a_2 is obtained, we find all conflicting edges originating from unlocked vertices of a_2 , which is the first Type-2 edge from a_2 to a_1 , with shared location C_2 . From the speed profile of a_2 , we use the leave time $t_2^l(C_2)$ as the split time. We divide the time interval at C_2 into $[0, t_2^l(C_2)]$ and $(t_2^l(C_2), \infty)$. The reserved intervals of a_1 and a_2 are updated by intersecting their current reserved intervals with these segments, respectively. By assigning these intervals, the Type-2 edge is marked as satisfied. Any speed profile generated for a_2 in subsequent iterations must adhere to this updated interval.

We use the leave time as the split time to ensure that a feasible speed profile always exists when replanning for a_i in future iterations. Concretely, since, in the current iteration, the reserved intervals at the last unlocked vertex and all following locked vertices have an infinite upper bound, the next time when we replan a_i , a_i can follow the speed profile generated in the current iteration, wait at the last unlocked

vertex as needed, and continue without violating constraints.

4 kTPG with Uncertainty

In the previous section, we assumed the agents can perfectly follow the speed profiles. However, in realistic scenarios, agents may experience temporal uncertainty during movement due to slippage or controller variability. To address this, we first introduce an uncertainty model to represent these temporal deviations. We then present kTPGu (kTPG with Uncertainty), which extends kTPG to account for these uncertainties using a safety margin mechanism.

Definition 2 (MAEP under Uncertainty) We extend the MAEP in Definition 1 by incorporating an uncertainty model for movement. The expected time for a_i to move from q_i^k to q_i^{k+1} is denoted T_i^k . However, due to the temporal uncertainty, the actual move time includes a random noise modeled as a normal distribution with zero mean and variance proportional to the movement distance. Thus, the actual move time \hat{T}_i^k from q_i^k to q_i^{k+1} is given by:

$$\hat{T}_i^k = T_i^k + \mathcal{N}(0, (\varepsilon_i^k)^2), \quad (\varepsilon_i^k)^2 = K_i \cdot d_k^{k+1}, \quad (1)$$

where d_k^{k+1} is the distance between q_i^k and q_i^{k+1} , and K_i is an agent-specific hyper-parameter.

To prevent collisions resulting from temporal uncertainty, we introduce safety margins to extend kTPG. Intuitively, a safety margin is an extra time buffer added between reserved intervals at shared locations to account for early or delayed arrivals, ensuring agents remain collision-free.

Using our uncertainty model, we can represent the time a_i reaches a certain vertex v_i^k as a normal distribution:

$$t_i^r(v_i^k) = t_i^r(v_i^0) + \sum_{j=0}^{k-1} \hat{T}_i^j = \mathcal{N}(\mu_i^k, (\sigma_i^k)^2). \quad (2)$$

with $\mu_i^k = \mu_i^0 + \sum_{j=0}^{k-1} T_i^j$, $(\sigma_i^k)^2 = (\sigma_i^0)^2 + \sum_{j=0}^{k-1} (\varepsilon_i^j)^2$. The reach time at the first vertex v_i^0 is $\mathcal{N}(0, 0)$, as agents start precisely at $t = 0$. For a Type-2 edge (v_i^{m+1}, v_j^n) between agents a_i and a_j with $loc(v_i^m) = loc(v_j^n)$, the probability of maintaining its passing order is:

$$\begin{aligned} P(t_i^l(v_i^m) < t_j^r(v_j^n)) &= P(t_i^r(v_i^{m+1}) - t_j^r(v_j^n) < 0) \\ &= P(\mathcal{N}(0, (\sigma_i^{m+1})^2 + (\sigma_j^n)^2) < \Delta\mu) \\ &= F_{\mathcal{N}_{m+1}^n}(\Delta\mu). \end{aligned} \quad (3)$$

where $\Delta\mu = \mu_j^n - \mu_i^{m+1}$, $F_{\mathcal{N}_{m+1}^n}$ is the cumulative density function of $\mathcal{N}_{m+1}^n = \mathcal{N}(0, (\sigma_i^{m+1})^2 + (\sigma_j^n)^2)$. Since σ depends only on the travel distance, we can derive $F_{\mathcal{N}_{m+1}^n}$ given the paths of the agents. To ensure with probability at least P_d that the passing order is not violated, i.e., $P(t_i^l(v_i^m) < t_j^r(v_j^n)) \geq P_d$, we can derive:

$$\mu_j^n - \mu_i^{m+1} \geq F_{\mathcal{N}_{m+1}^n}^{-1}(P_d). \quad (4)$$

From Eq. (4), the passing order defined by a Type-2 edge is maintained with a probability greater than P_d if the expected leave time of a_i exceeds the expected reach time of a_j by at least $F_{\mathcal{N}_{m+1}^n}^{-1}(P_d)$. Thus, we introduce kTPGu to handle time uncertainty by adding a minimum time gap between

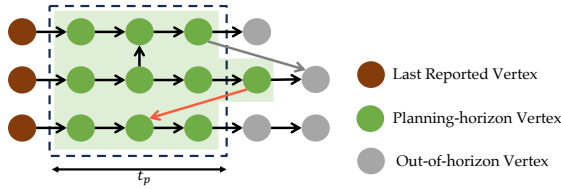


Figure 5: Illustration of the windowed robust execution.

the agents’ expected leave and reach times. Compared to the kTPG, the only modification is in updating reserved intervals. Once the leave time $t_i^l(v_i^m) = t_i^r(v_i^{m+1})$ for a_i at v_i^m is determined, we use Eq. (3) to compute the earliest time when a_j can reach v_j^n . The difference between $t_i^l(v_i^m)$ and $t_j^r(v_j^n)$ is referred to as the safety margin. Using this safety margin, we divide the time at $loc(v_i^m)$ into two intervals: $[0, t_i^r(v_i^{m+1})]$ for a_i and $(t_i^r(v_i^{m+1}) + F_{N_{m+1}^n}^{-1}(P_d), \infty)$ for a_j . These intervals are then intersected with the existing reserved intervals of a_i and a_j , resulting in updated reserved intervals for both agents, ensuring the passing order is maintained under time uncertainty.

5 Windowed kTPG (WinkTPG)

While adding safety margins ensures the speed profiles are collision-free with a certain probability, as shown in Eq. (2), the uncertainty in the reach times of an agent increases along its path. So, according to Eq. (4), the required safety margin for Type-2 edges between later vertices may become large, compromising solution quality. To address this, we propose using online execution information to reduce uncertainty.

Definition 3 (Real-Time MAEP under Uncertainty) *We extend the MAEP with uncertainty in Definition 2 by including information updates during execution, as proposed in (Hönig et al. 2019). We assume that agents report their actual reach times and current kinodynamic states upon arriving at each location.*

To maintain robustness while improving solution quality, we propose WinkTPG. WinkTPG periodically replaces the estimated reach times with the actual reach times reported by agents. Using these actual times, it recalculates the estimated reach times for subsequent vertices, reducing their uncertainty. WinkTPG employs a windowed replanning method (Berndt et al. 2023) to incorporate this updated information. Concretely, we trigger replanning every t_e seconds, during which we invoke kTPG_u to generate speed profiles within a defined planning window. A planning window, shown as the green region in Fig. 5, is a subset of the original TPG and spans at least t_p vertices for each agent.

When replanning is triggered, we follow the method from (Berndt et al. 2023) to determine which vertices to include in the planning window. For each agent, we identify its most recently reported vertex and the corresponding reach time. The next N_E vertices are then marked as *enqueued*, meaning the agent can continue to follow its previous speed profile through these vertices without replanning. The planning window begins immediately after the last

enqueued vertex. As shown in Fig. 5, we first include the next t_p vertices for each agent in the window. To ensure all precedence constraints are satisfied, we further check Type-2 edges within the window. If any such edge originates from outside the current window (e.g., the red edge in Fig. 5), we recursively expand the window to include the source vertex and any earlier vertices needed to preserve execution order.

Once the planning window is finalized, we use kTPG_u to compute speed profiles for all agents within it. Using the last reported vertex v_i^p and its corresponding reach time $t_i^r(v_i^p)$ for each agent, we calculate the updated reach time for subsequent vertices as: $t_i^r(v_i^k) = t_i^r(v_i^p) + \sum_{j=p}^{k-1} \hat{T}_j$. This reduces the temporal uncertainty in the estimated reach time. Once the speed profiles are generated, they are sent to the agents for execution. This replanning and execution process repeats until all agents reach their goals.

6 Theoretical Analysis

Theorem 1 (Completeness of kTPG and kTPG_u) *Given a collision-free MAPF plan, kTPG and kTPG_u return a feasible solution in finite time, though it may be suboptimal.*

Proof 1 *As shown in Section 3.4, our method of determining the split time ensures that we can always find a valid speed profile in each iteration. Since \mathcal{G} is guaranteed to be a directed acyclic graph (Hönig et al. 2016), if there are locked vertices in \mathcal{G} , there is at least one conflicting edge originating from an unlocked vertex to a locked vertex. So when we replan for the agent associated with this unlocked vertex, kTPG guarantees progress by satisfying at least this conflicting edge. Therefore, kTPG is guaranteed to unlock all vertices after a finite number of iterations. That is, kTPG is complete and guarantees to find feasible solutions. For kTPG_u, incorporating a safety margin does not affect the existence of a valid speed profile in each iteration, making the completeness of kTPG unchanged.*

Theorem 2 (Completeness of WinkTPG) *Given a collision-free MAPF plan, WinkTPG ensures that all agents reach their goal locations without collisions in finite time.*

Proof 2 *In each planning window, feasibility is ensured by allowing each agent to retain and follow its previously computed speed profile up to the last vertex from the previous window. Based on the reasoning in Section 3.4, we ensure that, for each agent, a valid speed profile exists for each agent in the current window, enabling it to wait at the final vertex of the previous window before proceeding. As shown in Theorem 1, at least one agent makes progress in each set of speed profiles. Thus, WinkTPG completes in finite time with a bounded number of kTPG_u calls.*

Theorem 3 (Time Complexity of kTPG and kTPG_u) *kTPG and kTPG_u require at most $\min(|\mathcal{V}|, |\mathcal{E}_2|)$ iterations of speed profile updates.*

Proof 3 *As proved in Theorem 1, each iteration satisfies at least one new Type-2 edge and unlocks at least one previously locked vertex. This implies that the total number of iterations is upper bounded by $\min(|\mathcal{V}|, |\mathcal{E}_2|)$. Since WinkTPG calls kTPG_u within each of the W planning windows, the total number of iterations is at most $W \cdot \min(|\mathcal{V}|, |\mathcal{E}_2|)$.*

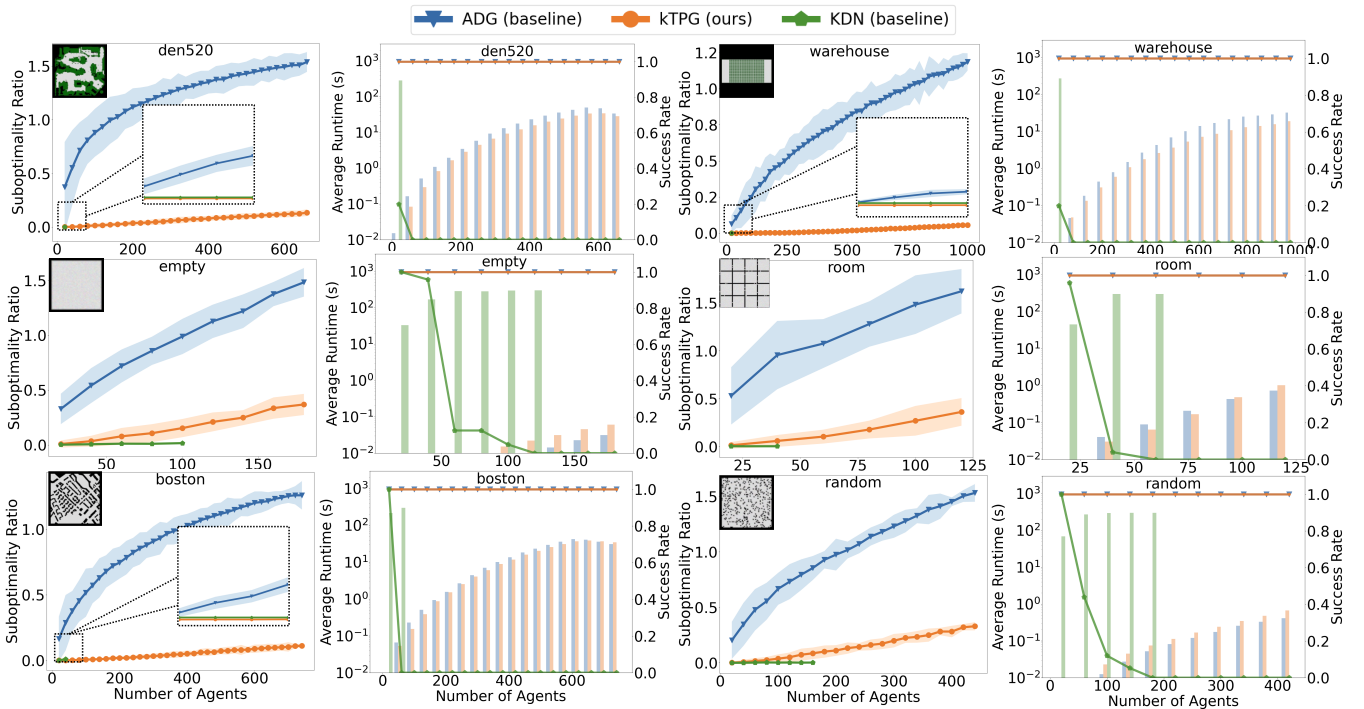


Figure 6: Average suboptimality (odd-numbered columns), average runtime (bar plots in even-numbered columns), and success rate (line plots in even-numbered columns).

7 Empirical Evaluation

All methods included in the study were implemented in C++ and tested on an Ubuntu 20.04 system with an AMD 3990x processor and 188 GB of memory. The code was run using a single core for all computations. The source code for our method will be publicly available upon acceptance.

We evaluate all methods on six four-neighbor grid maps from the MovingAI MAPF benchmark (Stern et al. 2019): empty (size: 32×32), random (size: 64×64), room (size: 64×64), den520d (size: 256×257), and Boston (size: 256×256), warehouse-large (size: 340×164). The distance between two neighboring grids is 1 m. The MAPF plans used for execution are generated by PBS (Ma et al. 2019). We use *suboptimality ratio* to evaluate the solution quality, which is defined as $\frac{T_{sum} - T_{ideal}}{T_{ideal}}$, where T_{sum} is the sum of reach times, and T_{ideal} is the sum of individual agent reach times without considering collisions or delays.

7.1 Kinodynamic Planning

In this experiment, we evaluate the solution quality of the speed profiles generated by kTPG and compare it against two baselines: ADG and KDN. ADG (Hönig et al. 2019) generates speed profiles by planning only for vertices without unsatisfied incoming Type-2 edges, using the same speed profile planner as kTPG. Furthermore, ADG is assumed to have access to real-time agent locations and replans its speed profile every 0.01s. KDN (Zhang et al. 2021) formulates the temporal dependency of TPG as a MILP problem and finds the optimal solution for Definition 1.

Experiment Setup Since KDN is designed for an omnidirectional robot model without uncertainty, we adopt the same setting in this experiment. An *omnidirectional robot* can move in any orientation, with its speed profile constrained by the dynamic limits of its physical model. In this experiment, each agent is subject to a speed limit of $[0, 2]$ m/s and an acceleration limit of $[-1, 1]$ m/s². As required by the speed profile planner, speeds at the vertices are discretized into three levels: $\{0, \sqrt{2}, 2\}$ m/s. The runtime limit for all methods is 300 seconds.

Result Analysis As shown in Fig. 6, both kTPG and KDN show significant improvements in solution quality across all maps compared to ADG. This improvement is more evident on larger maps with more agents (e.g., up to 51.7% in the warehouse map). This is because ADG only plans speed profiles for vertices without incoming Type-2 edges. In situations with more Type-2 edges, this strategy is overly conservative and leads to frequent unnecessary deceleration. While KDN achieves slightly better solution quality, it is much less scalable than kTPG. Both kTPG and ADG maintain a 100% success rate on problems involving up to 1,000 agents. In contrast, KDN, while ensuring optimality, cannot solve problems with more than 100 agents. This is due to KDN relying on a MILP formulation to encode the precedence constraints imposed by Type-2 edges, whose complexity grows exponentially with the number of Type-2 edges. Notably, while the runtime for each planning round of ADG is low, its frequent replanning significantly increases the total runtime, making it similar to that of kTPG.

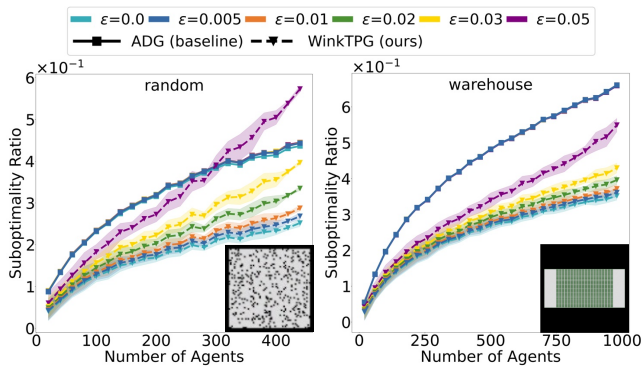


Figure 7: Comparison of solution cost between ADG (dashed lines) and WinkTPG (solid lines) across different uncertainty levels (indicated by color). The ADG lines largely overlap across uncertainty levels in both figures.

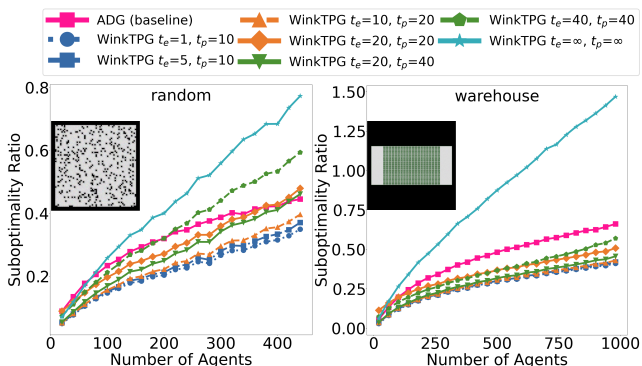


Figure 8: Comparison of solution cost between ADG and WinkTPG, with different execution and planning window.

7.2 Robust Execution Under Uncertainty

In this section, we evaluate the performance of WinkTPG in environments with temporal uncertainty. As KDN cannot handle uncertainty, only ADG is used as a baseline.

Experiment Setup We use a differential-drive robot model that is more commonly used in real-world applications. Compared to omnidirectional robots, it moves only along its current orientation, while being constrained by the same dynamic constraints as in the previous section. It can change its orientation only when its velocity is zero. Specifically, it takes 0.5 s to turn left or right and 0.9 s to turn backward. We set the safety probability threshold to $P_d = 0.99$ and use $K_i = \varepsilon^2$ for all agents, where ε is a hyperparameter. By Eq. (1), the variance of the move time to an adjacent vertex is $(\varepsilon_i^k)^2 = \varepsilon^2$ as the move distance is 1 m. We use different ε values to model different uncertainty levels. For intuition, given a movement between two adjacent vertices, its expected move time is $\frac{1\text{m}}{2\text{m/s}} = 0.5\text{ s}$. For $\varepsilon = 0.05$, by applying the 3- σ rule (Casella and Berger 2024), it implies there is up to $\pm 30\% \times 0.5\text{ s}$ uncertainty in move time. Given this level of noise is already substantial for short-range motion, we limit ε to values no greater than 0.05.

Table 1: Planning Runtime (in seconds) on the warehouse map with $\varepsilon = 0.03$. MAPF refers to the time taken to generate the initial MAPF plan, while ADG and WinkTPG represent the runtime per planning round.

Agents #	MAPF	ADG	WinkTPG	
			$t_p=10\text{ s}$	$t_p=\infty$
100	0.089 ± 0.03	2.36 ± 0.29 $\times 10^{-4}$	$t_p=10\text{ s}$	0.002 ± 0.00
			$t_p=20\text{ s}$	0.003 ± 0.00
			$t_p=40\text{ s}$	0.005 ± 0.00
			$t_p=\infty$	0.266 ± 0.05
1,000	44.51 ± 3.94	2.02 ± 0.09 $\times 10^{-3}$	$t_p=10\text{ s}$	0.344 ± 0.01
			$t_p=20\text{ s}$	0.389 ± 0.01
			$t_p=40\text{ s}$	0.519 ± 0.02
			$t_p=\infty$	28.21 ± 1.67

Result Analysis We first evaluate WinkTPG under varying uncertainty levels using a fixed window size. Specifically, the execution window t_e is set to 10 s, and the planning window t_p is 20. As shown in Fig. 7, while WinkTPG generates more suboptimal solutions with larger ε , it consistently outperforms ADG in environments with moderate temporal uncertainty (i.e., $\varepsilon < 0.03$). This supports our earlier claim that ADG is an overly conservative strategy. The solution quality of ADG remains nearly constant across different uncertainty levels because it replans at a very high frequency and is thus less sensitive to temporal uncertainty. As shown later, WinkTPG also achieves better solution quality with a smaller execution window.

Next, we evaluate the relationship between solution quality and the length of the execution and planning windows. All experiments are conducted in environments with $\varepsilon = 0.03$. As shown in Fig. 8, configurations where the execution window is smaller than the planning window consistently show better solution quality. Also, smaller execution windows always achieve better performance, due to more frequent replanning with updated location information.

Finally, we report in Table 1 the runtime of ADG, WinkTPG, and the MAPF planner. In both cases, ADG and WinkTPG demonstrate significantly faster runtimes compared to the MAPF planner used to generate the paths. Notably, while ADG appears faster, it requires significantly more frequent replanning. Additionally, with an appropriately chosen planning window size, WinkTPG generates plans in under a second, showing it is capable of near real-time performance.

8 Conclusion

We introduced WinkTPG, an execution framework for efficiently and robustly executing MAPF plans in environments with execution uncertainty. WinkTPG uses our proposed kinodynamic planning method kTPG to generate collision-free speed profiles for all agents. It incorporates location updates from agents to replan dynamically while ensuring robust execution. We evaluated our methods in the MAPF domain, showing up to 51.7% improvement in solution quality compared to existing methods, while generating speed profiles for up to 1,000 agents in 1 second. Future work includes exploring the integration of WinkTPG with advanced MAPF replanning techniques such as rolling-horizon conflict resolution (Li et al. 2021) or switchable TPG (Feng et al. 2024).

References

- Ali, Z. A.; and Yakovlev, K. 2023. Safe Interval Path Planning with Kinodynamic Constraints. In *Proceedings of the AAAI Conference on Artificial Intelligence*, volume 37, 12330–12337.
- Andreychuk, A.; Yakovlev, K.; Boyarski, E.; and Stern, R. 2021. Improving continuous-time conflict based search. In *Proceedings of the AAAI Conference on Artificial Intelligence*, volume 35, 11220–11227.
- Atzmon, D.; Stern, R.; Felner, A.; Wagner, G.; Barták, R.; and Zhou, N.-F. 2020. Robust multi-agent path finding and executing. *Journal of Artificial Intelligence Research*, 67: 549–579.
- Berndt, A.; Van Duijkeren, N.; Palmieri, L.; Kleiner, A.; and Keviczky, T. 2023. Receding horizon re-ordering of multi-agent execution schedules. *IEEE Transactions on Robotics*, 40: 1356–1372.
- Casella, G.; and Berger, R. 2024. *Statistical inference*. CRC press.
- Feng, Y.; Paul, A.; Chen, Z.; and Li, J. 2024. A real-time rescheduling algorithm for multi-robot plan execution. In *Proceedings of the International Conference on Automated Planning and Scheduling*, volume 34, 201–209.
- Hönig, W.; Kiesel, S.; Tinka, A.; Durham, J. W.; and Ayanian, N. 2019. Persistent and robust execution of MAPF schedules in warehouses. *IEEE Robotics and Automation Letters*, 4(2): 1125–1131.
- Hönig, W.; Kumar, T. K. S.; Cohen, L.; Ma, H.; Xu, H.; Ayanian, N.; and Koenig, S. 2016. Multi-agent path finding with kinematic constraints. In *Proceedings of the International Conference on Automated Planning and Scheduling*, volume 26, 477–485.
- Li, J.; Hoang, T. A.; Lin, E.; Vu, H. L.; and Koenig, S. 2023. Intersection coordination with priority-based search for autonomous vehicles. In *Proceedings of the AAAI Conference on Artificial Intelligence*, volume 37, 11578–11585.
- Li, J.; Ruml, W.; and Koenig, S. 2021. EECBS: A bounded-suboptimal search for multi-agent path finding. In *Proceedings of the AAAI Conference on Artificial Intelligence*, volume 35, 12353–12362.
- Li, J.; Tinka, A.; Kiesel, S.; Durham, J. W.; Kumar, T. S.; and Koenig, S. 2021. Lifelong multi-agent path finding in large-scale warehouses. In *Proceedings of the AAAI Conference on Artificial Intelligence*, volume 35, 11272–11281.
- Liu, C.; Zhan, W.; and Tomizuka, M. 2017. Speed profile planning in dynamic environments via temporal optimization. In *2017 IEEE Intelligent Vehicles Symposium (IV)*, 154–159.
- Ma, H.; Harabor, D.; Stuckey, P. J.; Li, J.; and Koenig, S. 2019. Searching with consistent prioritization for multi-agent path finding. In *Proceedings of the AAAI Conference on Artificial Intelligence*, volume 33, 7643–7650.
- Moldagalieva, A.; Ortiz-Haro, J.; Toussaint, M.; and Hönig, W. 2024. db-CBS: Discontinuity-bounded conflict-based search for multi-robot kinodynamic motion planning. In *Proceedings of the IEEE International Conference on Robotics and Automation*, 14569–14575.
- Morris, R.; Pasareanu, C. S.; Luckow, K.; Malik, W.; Ma, H.; Kumar, T. S.; and Koenig, S. 2016. Planning, scheduling and monitoring for airport surface operations. In *AAAI Workshop: Planning for Hybrid Systems*.
- Okumura, K.; Machida, M.; Défago, X.; and Tamura, Y. 2022. Priority inheritance with backtracking for iterative multi-agent path finding. *Artificial Intelligence*, 310: 103752.
- Peltzer, O.; Brown, K.; Schwager, M.; Kochenderfer, M. J.; and Sehr, M. 2020. STT-CBS: A conflict-based search algorithm for multi-agent path finding with stochastic travel times. *arXiv preprint arXiv:2004.08025*.
- Stern, R.; Sturtevant, N. R.; Felner, A.; Koenig, S.; Ma, H.; Walker, T. T.; Li, J.; Atzmon, D.; Cohen, L.; Kumar, T. K. S.; Boyarski, E.; and Barták, R. 2019. Multi-Agent Pathfinding: Definitions, Variants, and Benchmarks. In *Proceedings of the International Symposium on Combinatorial Search*, 151–159.
- Wurman, P. R.; D’Andrea, R.; and Mountz, M. 2008. Coordinating hundreds of cooperative, autonomous vehicles in warehouses. *AI magazine*, 29(1): 9–9.
- Yan, J.; and Li, J. 2024. Multi-Agent Motion Planning With Bézier Curve Optimization Under Kinodynamic Constraints. *IEEE Robotics and Automation Letters*, 9(3): 3021–3028.
- Zhang, H.; Tiruvilumala, N.; Koenig, S.; and Kumar, T. S. 2021. Temporal reasoning with kinodynamic networks. In *Proceedings of the International Conference on Automated Planning and Scheduling*, volume 31, 415–425.